JOURNAL OF MATERIALS SCIENCE 6 (1971) 395–402

Dislocation Etch Pits and Growth of Arsenic-Antimony Single Crystals

Y. C. AKGÖZ, G. A. SAUNDERS
Department of Applied Physics and Electronics, Science Laboratories, University of Durham, South Road, Durham, UK

Single crystals of an arsenic-antimony solid solution have been grown at the minimum melting point (612° C) composition (25.5 at.% arsenic) where the solidus and liquidus touch. Pyramidal etch pits produced on (111) cleavage faces mark the sites of emergence of dislocations; dislocation densities are low, ranging between 10^3 and 10^5 per cm^2. The relationship between an unambiguous, right handed axial set and etch pit orientation on the (111) surface is established. The permissible Burgers vectors and dislocation reactions are detailed and are related to the observed etch pit types. In general, the results obtained also apply to the A7 structure elements themselves and amend previous findings of the crystallographic relationships between dislocation directions and etch pits.

1. Introduction

Single crystals of arsenic-antimony alloys have been grown to fulfil sample requirements for measurements – now in progress – of the low field magnetoresistivity tensor. Since transport properties of alloys in general and, in particular, of semimetallic (or semiconducting) alloys, can be dominated by crystal perfection, emphasis has been placed on growth of high quality, single crystals and on examination of their perfection. An etch has been developed which produces pits on (111) surfaces exposed by cleavage. The character of these etch pits has been studied and their structure and crystallographic orientation is reported. Like the parent elements, the arsenic-antimony alloys take the A7 crystal structure; fig. 1 shows the primitive rhombohedral unit cell and primitive translation vectors $\mathbf{a}_1$, $\mathbf{a}_2$ and $\mathbf{a}_3$. The lattice parameter a and the rhombohedral angle α and thus the lattice distortion change monotonically throughout the arsenic-antimony alloys series [1]. In such crystals etch pits on the (111) cleavage plane have a unique orientation with respect to a right-handed $+x$, $+y$, $+z$ cartesian axial set; this relationship has been established.

A variety of tests has been used to demonstrate that the etch pits mark the sites of emergence of dislocations on the (111) plane; etch pit counts show that the dislocation densities in the crystals are low for a metal alloy. Certain deviations from a perfect one-to-one correspondence between etch pits on opposite cleavage faces evidence bending and branching of the dislocations. Using the criterion that the self-energy of a dislocation line is proportional to the square of the Burgers vector, the possible dislocation reactions and the stability of dislocations in the alloy crystals are discussed. Previous workers on etch pits in A7 structure crystals have tended to use an erroneous definition of a right-handed, orthogonal axial set. As a result the basic crystallographic directions have not been assigned correctly. The present work on the arsenic-antimony alloys includes, as far as we are aware, the first treatment of basic dislocation line directions and Burgers vectors in the proper crystallographic framework for this structure; the general results obtained also hold for crystals of the parent elements themselves.

2. Crystal Growth

A continuous series of solid solutions is formed between arsenic and antimony. Parravano and de Cesaris [2] found a minimum melting point (612° C) for the composition containing 25.5 at. % arsenic; although more recent workers have suggested somewhat different compositions for the minimum melting point alloy, an extensive study [3] has confirmed the earliest work. The solidus and liquidus touch at the minimum melting point, liquid and solid phases of this composition alone in the solid solution series are

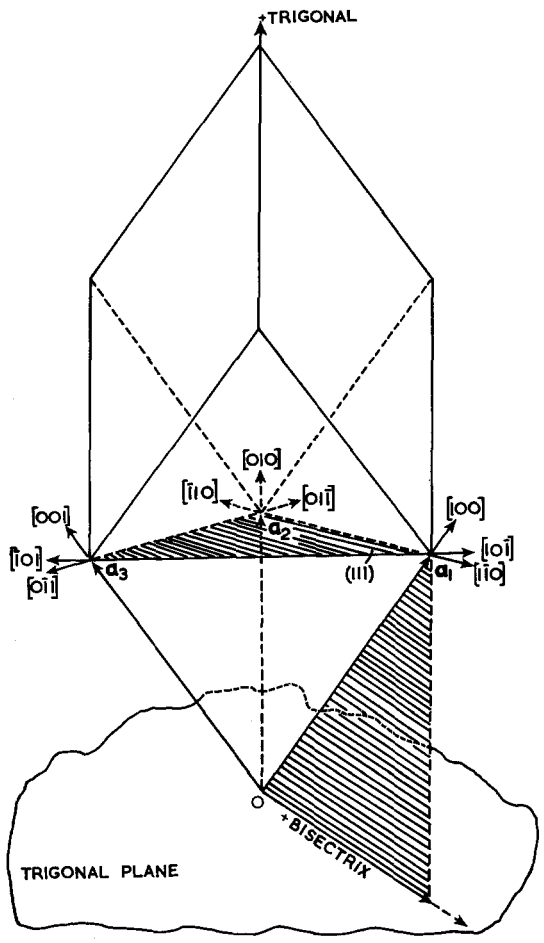

Figure 1 The primitive rhombohedral unit cell of the A7 structure; the primitive translation vectors are denoted by $\mathbf{a}_i$ ($i = 1, 2, 3$). The standard co-ordinate system is illustrated: the + y axis is chosen by projecting one of the $\mathbf{a}_i$ onto the trigonal plane and then the positive direction taken outwards from the origin 0 of the $\mathbf{a}_i$. The $\langle 10\bar{1} \rangle$ directions on the (111) cleavage plane which delineate the slip lines are shown.

in equilibrium, and a liquid of this composition will freeze to a solid of the same composition. Major problems can arise in growing single crystals of solid solutions because usually the solid and liquid phases in equilibrium at a given temperature do not have the same composition; a variety of crystalline imperfections result, including, on a gross scale, concentration gradients along the boule or cell-like substructure or dendritic formation due to constitutional supercooling. Inhomogeneities can dominate both carrier mobilities and densities in a semimetal or semiconductor and result in non-intrinsic, anomalous galvanomagnetic effects [4, 5]. In the case of the arsenic-antimony solid solutions, growth at the minimum melting point composition avoids these problems. Thus this particular alloy is a most suitable vehicle for studies of the fundamental electron transport properties. The present concern is to discuss the growth and perfection of crystals of this composition.

Single crystals of arsenic (25.5 at. %, 17.4 wt. %)- antimony alloys were grown from 99.99% purity elements by a modified Bridgman technique. Evacuated (10^{-4} torr), 16 mm internal diameter, quartz growth tubes with thick walls (1.6 mm), on account of the substantial vapour pressure of arsenic, were employed. Use of a single pointed end on the growth tube proved as satisfactory as employment of a constricted tube for single seed selection. A 20 mm length of 3 mm quartz rod was fused to the end of the growth tube as a spacer, because direct contact with the steel support rod used in the furnace destroyed the temperature gradient at the tip, in which case several longitudinal crystals grew. To reduce oxidation, the arsenic was bought in sublimed form in evacuated tubes containing a suitable quantity for one run. The arsenic was weighed and transferred immediately to the growth tube (containing the antimony) and put under vacuum at once. Heating to 350°C under vacuum for 3 h distilled off any volatile oxide present; the growth tube was then sealed off. The growth furnace used has been detailed elsewhere [6, 7]; Gouy modulation was incorporated in a switching galvanometer controller to stabilise the temperature to within $\pm$ 0.2°C. A series of experiments showed that the best crystals were obtained by maintaining the temperature gradient at 10°C/cm near the freezing interface and using a crystal growth rate of 2 mm h^{-1}.

Arsenic and antimony single crystals tend to grow with the z-axis nearly normal to the growth direction; but the z-axis of the alloy crystals is directed randomly between 50° and 75° with respect to the growth axis. As a rule, A7 structure crystals cleave readily to expose (1 1 1) faces; the arsenic-antimony alloys are no exception. The crystals show a perfect cleavage on the (1 1 1) face. Unlike arsenic, the alloy does not oxidise markedly on prolonged exposure to the air, and cleaved surfaces retain their shiny appearance. Back reflection Laue X-ray photographs yield pin-point spots with no trace of

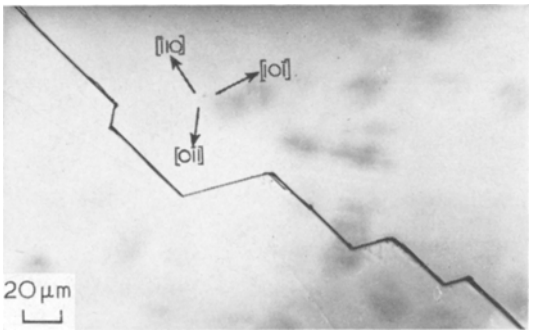

Figure 2 Slip lines on a cleaved, unetched, (111) surface of an arsenic-antimony single crystal. Three sets of lines mutually oriented at 120° and parallel to $\langle 10\bar{1} \rangle$ directions can be seen.

spreading, asterism or splitting: a useful first indication of high perfection. Debye-Scherrer powder photographs of this 25.5 at. % alloy show that the primitive rhombohedral lattice parameter a is equal to 4.418 ± 0.001 Å and α is equal to 56° 12′ ± 3′. Further studies have been made by etch pit techniques.

3. Dislocation Etch Pits in Arsenic-Antimony Alloys

Microscopic examination of (111) cleaved surfaces of the alloy crystals discloses the same sets of straight slip lines (fig. 2), mutually orientated at 120°, as those found in crystals of arsenic, antimony, and bismuth. These slip lines are rarely observed in the more perfect alloy crystals after careful cleaving. The symmetry elements of the A7 crystal structure comprise three diad (x) axes normal to three mirror (yz) planes, mutually orientated at 120°, which intersect in the inversion triad (z). Bisectrix (y) axes, one in each mirror plane, complete three possible orthogonal (x, y, z) axial sets. The slip line system on the cleaved surface reflects this symmetry; three sets of slip lines are seen, each parallel to one of the three possible choices of binary (x) axes. The primary slip system comprises the (111) as glide plane and the $\langle 10\bar{1} \rangle$ as slip directions (see fig. 1 for the geometry), and this system cannot give rise to slip lines on the (111) plane. The slip lines seen delineate the intersection along the $\langle 10\bar{1} \rangle$ directions of each of the three possible secondary slip planes $\{10\bar{1}\}$ with the (111) plane. The deformation is such that the crystal orientation is retained on either side of the slip lines; the etch pits do not invert across the slip lines (fig. 3). No exceptions to this rule have been found: this does seem to be deformation by slip, not twinning.

Several potential etching reagents were examined; an etch composed of three parts hydrofluoric acid (40 %), five parts concentrated nitric acid, three parts glacial acetic acid and a few drops of bromine, aged for one month in an enclosed container, was the most successful. After immersion of the crystal for one to two seconds, followed by washing in distilled water, this etch produced pits on the (111) cleavage plane which were much better defined than is usual in metal alloys. The pits are triangular with slightly rounded corners and have pyramidal bottoms; some are symmetrical with the pit apex

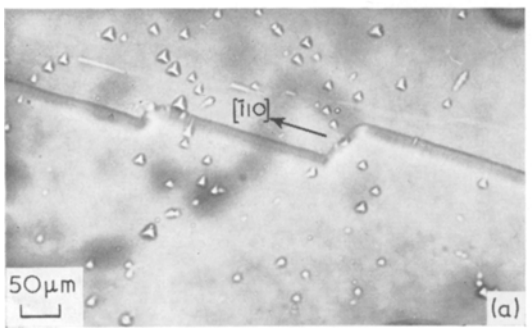

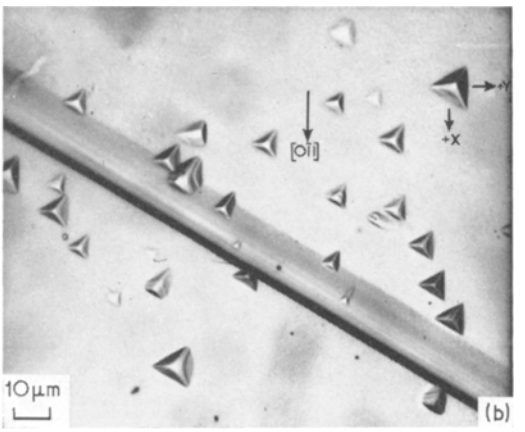

Figure 3 The relationship between etch pit orientation and slip lines. (a) A region of multiple slip after etching. This is actually part of the slip line system shown in fig. 2. Traces of etch grooves are also visible, some end in small etch pits. (b) Higher magnification to show the pyramidal etch pits and one slip line. The etch pit orientation is shown with respect to an orthogonal (+ x, + y, + z) axial set (+ z is directed normally out from the plane of the photograph).

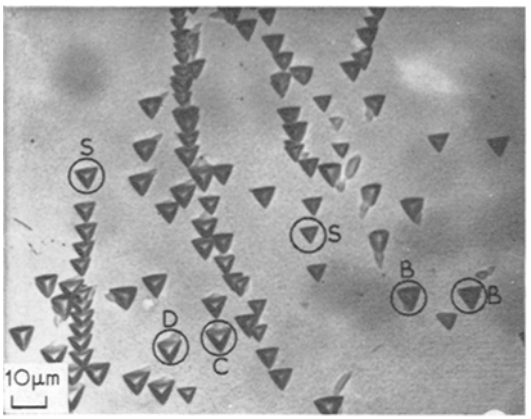

Figure 4 A variety of different types of pit: symmetrical (S), asymmetrical with projected apex deflected (B) towards a base (C) towards a corner and (D) completely asymmetric.

below the centre of the etch pit triangle, in others the apex is sited either towards one side or a corner (fig. 4). It is appropriate to discuss the reason for this later. The pit sides are parallel to the $\langle 10\bar{1} \rangle$ crystallographic directions and, in consequence, to one of the slip line systems. This pit shape on the (1 1 1) cleavage plane is common to several $R\bar{3}m$ crystals: bismuth [8], antimony [9], arsenic [6, 10], Bi_2Te_3 [11, 12]. Hexagonal etch pits can be produced on the (1 1 1) plane of arsenic [6] and Bi_2Te_3 [11, 12], but not in the case of antimony or of the arsenic-antimony alloy; that both trigonal and hexagonal pits can be found in arsenic and Bi_2Te_3, probably results from their layer-like crystal structures [6].

The well-defined shape of the etch pits suggests that they mark the sites of emergence of dislocations of the (1 1 1) plane, as in bismuth [8], antimony [9], arsenic [6,10] and Bi_2Te_3[11, 12]. Several techniques are available for testing this suggestion and we have used those listed below. (*a*) On successive etching the pits enlarge but retain their shapes (fig. 5). For the most part the pit numbers, appearance and overall pattern remain unaltered on prolonged etching. But there are certain changes which in themselves lead to much useful information. A few new smaller pits with the typical pointed apex do form (shown by the arrows); also some of the original pits develop flat bottoms (fig. 5d): the dislocation

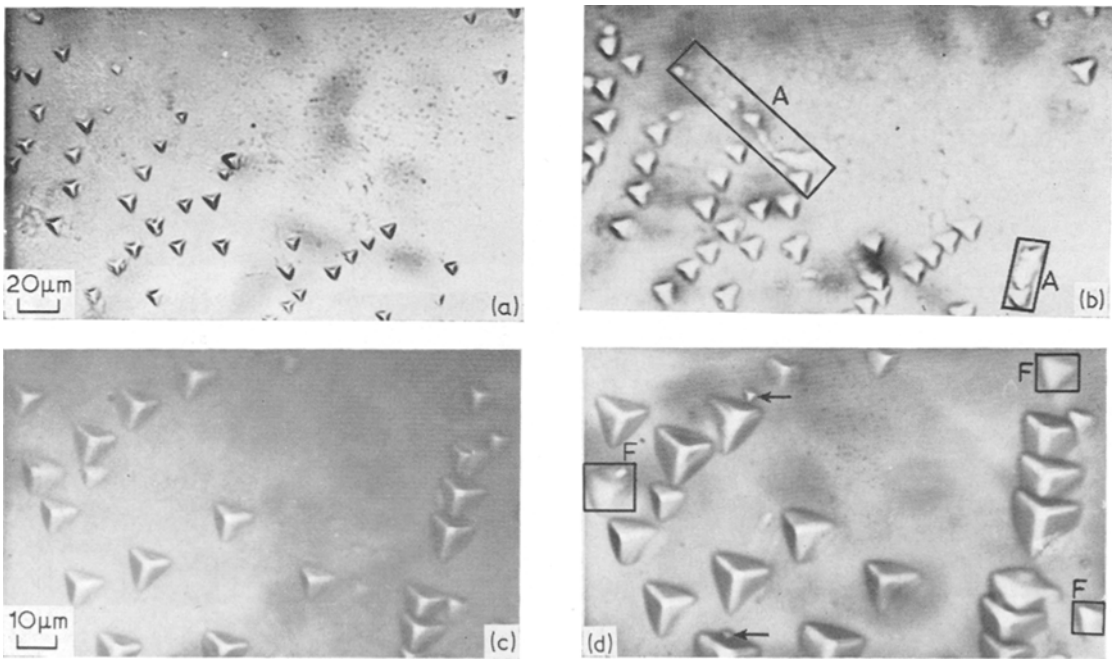

Figure 5 To show the effects of successive etching (a) after 1 sec, (b) after 3 secs. Etch pits enlarge and keep their shape. Usually there is a one-to-one correspondence of etch pits. Etch grooves can develop after successive etching (see inside the rectangles A in (b)). Other features which develop on successive etching are illustrated in the pair of photographs (c) (after 2 secs) and (d) (after 3 secs). New small pyramidal pits can develop (shown by the arrows); usually these are related closely with an original pit. Some of the original pits develop flat bottoms: examples are shown in the squares labelled F.

line no longer lies in the pit. Extended dislocation networks lying in the basal plane are revealed as shallow etch grooves. On prolonged etching, small pits are sometimes found in association with the end of an etch groove (see A in fig. 5b). Similar observations have been made in etch pit studies in Bi_2Te_3 [11, 12] and interpreted on the basis of dislocation branching or bending near the surface.

(*b*) A second test for the reliability of an etch for revealing dislocations is to establish a one-to-one correspondence between the etch patterns obtained on opposite faces of a cleaved crystal. Fig. 6 shows that the etch patterns on opposite faces do match for the most part, although they exhibit inversion symmetry with respect to each other. Such an inversion should be present in materials with an appropriate inversion axis normal to the plane on which the etch pits are produced and is found for arsenic, antimony and bismuth as well as for the arsenic-antimony alloys, although there is some confusion in the literature over this point. The match on opposite faces is not always perfect for the arsenic-antimony alloy crystals, nor is it for Bi_2Te_3 [11, 12] or arsenic [6]. Extra features on one face can result from bending or branching of a dislocation close to the plane of cleavage [12]. A groove accompanying an extra pit on one face clearly establishes dislocation bending near the cleavage (G in fig. 6a and b). The discrepancies from one-to-one correspondence of etch pits noted after both prolonged etching (fig. 5) and matched face (fig. 6c and d) experiments need not detract from the reliability of the etch for revealing the sites of emergence of dislocations. Rather they add weight to the proposition.

(*c*) The etch reveals rows of pits on the (1 1 1) cleavage planes (fig. 7), particularly in less perfect crystals grown especially to allow investigation of this feature. Similar rows of pits found in antimony [9], bismuth [8] and arsenic [6] are known to mark dislocation tilt boundaries. For the arsenic-antimony alloy crystals, etch pit counts along pit rows near intersections demonstrate that these rows mark tilt boundaries. Successive cleaving and etching experiments on crystals of thicknesses between 0.1 and 1 mm show that the general pattern of low angle grain boundaries is preserved throughout large regions of these crystals. More marked changes are found in the individual etch pit positions.

These tests evidence that the etch used does reveal the sites of emergence of dislocations on

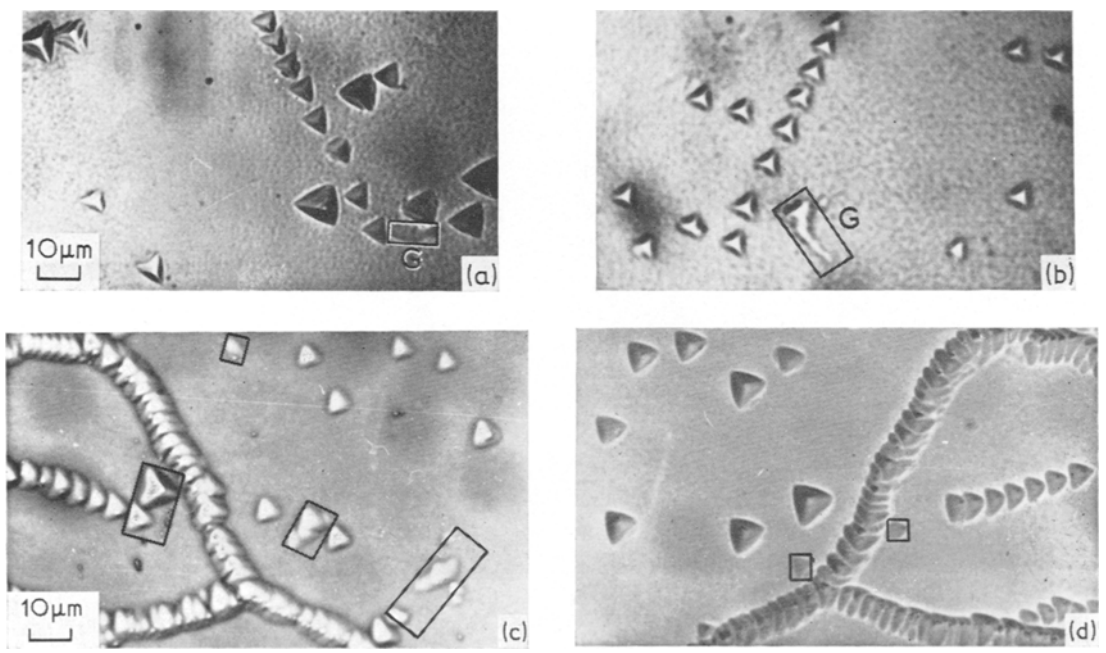

Figure 6 Etch pits match on opposite cleaved faces except for the inversion. (a) and (b) are one matched pair and (c) and (d) another. One-to-one correspondence is usual. Extra etch grooves (G) can be seen in (a) and (b). In many cases certain pits can be seen on only one of a pair of faces; examples are marked in (c) and (d).

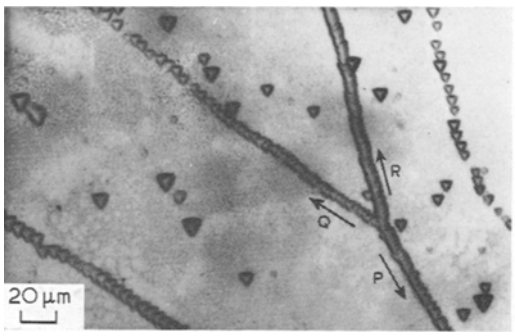

Figure 7 Intersecting low angle grain boundaries.

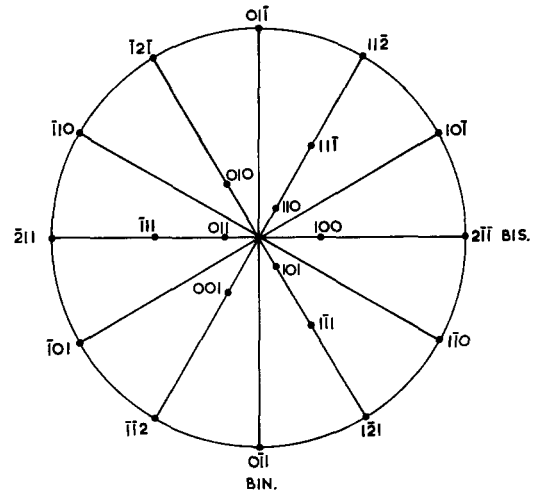

Figure 8 Standard (111) stereographic projection for directions in the arsenic-antimony alloy, showing directions of particular interest to dislocation studies in this material.

the (1 1 1) cleavage face. Most of the crystals have etch pit counts of between 10^4 and 10^5 per square cm; the best crystals have counts as low as 10^3 per square cm. At the boule sides, where the growth tube touches, the dislocation density is about an order of magnitude greater than in the main body of the crystal. These findings point to remarkably low dislocation densities for a metal solid solution and substantiate the method of growth and the use of this alloy for fundamental studies of electron transport.

Specimens were indented using a Vickers microhardness tester and then etched. No new etch pits were evident. It can be concluded that at room temperature arsenic-antimony alloys are brittle and that the dislocation mobility is essentially zero.

To proceed further and relate the etch pit structure with possible dislocations, it is necessary to consider the permissible Burgers vectors and dislocation reactions for the A7 crystal structure. A standard (1 1 1) projection, including those directions particularly relevant to dislocation studies, is shown in fig. 8. Parameters associated with dislocations most likely to occur are collected in table I. The self-energy of a dislocation line is proportional to the square of the Burgers vector (**b**) which is presented in table I both for the A7 structure in general and for the arsenic-antimony alloy having a rhombohedral angle α equal to 56° 12′ in particular. The sense of the angle that the Burgers vector makes with the [1 1 1] direction can be found from the stereographic projection in fig. 8 and the magnitude of this angle from table I. The Frank stability rule can now be used to determine which dislocations are most likely to be stable; dislocations of large **b** can lower their energies by spontaneous dissociation: a dislocation $\mathbf{b}_1$ will dissociate into two dislocations $\mathbf{b}_2$ and $\mathbf{b}_3$, if $b_1^2 > (b_2^2 + b_3^2)$, that is if $\mathbf{b}_2.\mathbf{b}_3 > 0$. Therefore, the lowest energy dislocation should have a

TABLE I Possible dislocations in the A7 crystal structure in general and in the 25.5 at.% arsenic-antimony alloy in particular.

Burgers vector (**b**)	No. of equivalent Burgers vectors	$\|\mathbf{b}\|^2$	Angle between (**b**) and [111]
$\langle 10\bar{1}\rangle$	6	$4a^2 \sin^2 \frac{\alpha}{2} = 0.88\, a^2$	90°
$\langle 100\rangle$	6	a^2	33°
$\langle 1\bar{1}1\rangle$	6	$a^2\left(1 + 4 \sin^2 \frac{\alpha}{2}\right) = 1.88\, a^2$	52°
$\langle 110\rangle$	6	$4a^2 \cos^2 \frac{\alpha}{2} = 3.11\, a$	18°
$\langle 111\rangle$	2	$3a^2\left(1 + 4 \cos^2 \frac{\alpha}{2}\right) = 6.34\, a^2$	0°

Burgers vector equal to the smallest Bravais lattice vector; other small values of **b** can also lead to stable dislocations. These criteria evidence that dislocations with Burgers vectors $\langle 10\bar{1}\rangle$, $\langle 100\rangle$ or $\langle 1\bar{1}1\rangle$ are stable in the A7 structure. Energy is balanced on both sides of the reactions:

(1) $[1\bar{1}1] \rightarrow [1\bar{1}0] + [001]$
Energy proportional to $1.88a^2 \quad 0.88a^2 \quad a^2$

It is not possible to decide on this elementary theoretical basis which direction this particular reaction takes, but in the case of dislocations with Burgers vectors $\langle 110\rangle$ or $[111]$ a reduction in energy can accrue through the reactions:

(2) $[110] \rightarrow [100] + [010]$
Energy proportional to $3.11a^2 \quad a^2 \quad a^2$
Energy reduction = 36%

(3) $[111] \rightarrow [110] + [001]$
Energy proportional to $6.34a^2 \quad 3.11a^2 \quad a^2$
Energy reduction = 35%

(4) $[111] \rightarrow [100] + [010] + [001]$
Energy proportional to $6.34a^2 \quad a^2 \quad a^2 \quad a^2$
Energy reduction = 53%

Thus decomposition of these dislocations is energetically favourable. Two dislocations can combine to form a single dislocation; dislocation reactions likely to onset at the intersection of slip systems include [10]:

(5) $[00\bar{1}] + [100] \rightarrow [10\bar{1}]$
Energy proportional to $a^2 \quad a^2 \quad 4a^2 \sin^2 \frac{\alpha}{2} = 0.88a^2$
Energy reduction = 56%

(6) $[\bar{1}01] + [1\bar{1}0] \rightarrow [0\bar{1}1]$
Energy proportional to $0.88a^2 \quad 0.88a^2 \quad 0.88a^2$
Energy reduction = 50%

The task remaining is to collate the different kinds of pit with the permissible stable dislocations and thus assess which dislocations may actually be present. The way in which specific dislocations could lead to certain asymmetrical etch pits was touched upon for antimony by Kosevich [13] and the general approach extended by Shetty and Taylor [10] in their studies on arsenic. A similar approach is used here for the arsenic-antimony alloys. However, it must be pointed out that the previous work on antimony and arsenic suffers from incorrect definition of a right-handed, orthogonal axial set for the crystals; actually an axial set is not defined in either study, but careful examination of the micrographs and the crystallographic directions used indicates that a faulty definition has been tacitly assumed. An important point this: there has been a general tendency to use a wrong axial assignment in etch pit and dislocation studies in all the A7 structure materials. The error still persists: notably, a recent paper on bismuth [14] shows a drawing of an etch pit on which the wrong axial set is clearly marked. The standard co-ordinate system is illustrated in fig. 1, the bisectrix (y) axis, for which three options obtain, is defined by projecting one $\mathbf{a}_i$ on to the trigonal plane and choosing the $+y$ direction outwards from the origin 0 of the $\mathbf{a}_i$ [15, 16]; a $+x$ axis then completes the right-handed orthogonal set. A $(+x, +y, +z)$ axial set has been assigned unambiguously to the crystals under investigation here by use of Laue back reflection photographs (the $+y+z$ quadrant in the mirror plane contains a pseudo-threefold axis and the $-y+z$ quadrant a pseudo-fourfold axis). The orientation of the etch pits with respect to the $+x$ and $+y$ axis on the (111) plane has then been determined. In the arsenic-antimony alloy the etch pits obey the same rule as those in arsenic and antimony themselves [17]: a vector drawn from the pit centre normal to a pit side points along the $+y$ axis, when the outward normal from the cleaved surface is taken as the $+z$ direction (fig. 3b). Once this is known the crystals can be orientated by a simple visual inspection after cleaving and etching; first the $+z$ axis is defined, the $+y$ axis is then found from the etch pits, and finally the x direction found accurately from the slip lines. This technique is useful because the signs of the components of many tensor properties depend upon the definition of a right-handed $(+x, +y, +z)$ axial set in the particular crystal under investigation [15-20]. For example, the signs of A_{42} and A_{24} of the magnetoresistivity tensor [16, 18, 19] and of C_{14} of the elastic stiffness tensor [15, 17], or the orientation dependence of the Umkehr effect [20] depend upon this assignment.

Several distinct types of pyramidal etch pits have been observed in the arsenic-antimony alloys (fig. 4). Symmetrical pits occur together with asymmetrical pits in which the projected apex is deflected, either towards a base or a

corner of the etch pit triangle. These pit types can now be related to the permissible stable dislocations. Inspection of micrographs of antimony and arsenic taken previously in this laboratory and those in references [10] and [13], shows that the arguments set out below are valid for the pure elements as well as for the arsenic-antimony alloy. But arsenic and antimony themselves need not be discussed in detail here. The symmetrical pits are probably formed by dissolution along dislocation lines running parallel to the *z*-axis; tentatively, it may be suggested that these are edge dislocations with one of the $\langle 10\bar{1} \rangle$ as Burgers vector which would be very stable (see table I) rather than the screw dislocations proposed by Kosevich [13] (a dislocation with a $\langle 111 \rangle$ Burgers vector is not likely to be stable in this structure, see table I and reactions 3 and 4).

A dislocation parallel to a $\langle 110 \rangle$ direction makes an angle of 18° with the [111] direction (fig. 8). Dissolution along this dislocation line would produce pits with the projected apex deflected towards one of the corners of the etch pit triangle (not towards one of the bases, as the erroneous definition of axes leads Kosevich [13] and Shetty and Taylor [10] to predict). Etch pits corresponding to this dislocation direction are not uncommon; an example can be seen inside the circle labelled C in fig. 4. Detailed measurements of the etch pit dimensions have been made to assess the angle to which the apex deflection corresponds. Etch pit depths (about 2 to 4 μm) have been measured by focusing the microscope at the surface and then at the apex, and finding the lens traverse distance. This cannot be done with great accuracy. The angle is estimated as $20° \pm 5°$, in reasonable agreement with the postulate that this particular pit type arises from dislocations lying parallel to $\langle 110 \rangle$ directions. For such a direction an edge dislocation with Burgers vector $\langle 10\bar{1} \rangle$ would be stable, while a screw dislocation would not (see table I and reaction 2).

A screw dislocation parallel to $\langle 1\bar{1}1 \rangle$ and thus at an angle of 52° to the $\langle 111 \rangle$ direction is also permissible on the basis of the Frank stability rule; such a dislocation would lead to pits with the projected apex deflected well towards a corner; no pits of this type could be found; plausibly, such dislocations decompose via reaction 1 into dislocations with **b** equal to $\langle 1\bar{1}0 \rangle$ and [001]. This finding points to the direction taken by reaction 1. Pits in which the projected apex is deflected in a complex manner towards both corner and base also occur (fig. 4; D). Are these formed from mixed dislocations?

The commonest type of asymmetrical etch pit is that in which the projected apex is deflected towards a base of the triangle. Measurements of the pit dimensions show that the angle which the associated dislocation makes with the [111] direction is $30° \pm 5°$. This angle and the sense of the apex deflection, point strongly to the mechanism of formation of this type of pit being dissolution along dislocations parallel to $\langle 100 \rangle$ directions which would make an angle of 33° with the [111] direction (see table I and fig. 8). This finding, coupled with energy considerations, suggests that screw dislocations of Burgers vector $\langle 100 \rangle$ are the most stable type of non-basal dislocation in the arsenic-antimony alloy and in arsenic and antimony themselves.

References

1. W. TRZEBIATOWSKI and E. BRYJAK, *Z. anorg. Chem.* **238** (1938) 255.
2. N. PARRAVANO and P. DE CESARIS, *Internat. Z. Metallog.* **2** (1912) 70.
3. B. J. SKINNER, *Econ. Geology* **60** (1965) 228.
4. R. T. BATE and C. A. BEER, *J. Appl. Phys.* **32** (1961) 800.
5. G. A. SAUNDERS, *Appl. Phys. Letters* **4** (1964) 138.
6. A. P. JEAVONS and G. A. SAUNDERS, *Brit. J. Appl. Phys. (J. Phys. D.)* Series 2, **1** (1968) 869.
7. A. P. JEAVONS, Ph.D. Thesis, University of Durham 1969.
8. L. C. LOVELL and J. H. WERNICK, *J. Appl. Phys.* **30** (1959) 234.
9. J. H. WERNICK, J. N. HOBSTETTER, L. C. LOVELL, and D. DORSI, *ibid* **29** (1958) 1013.
10. M. N. SHETTY and J. B. TAYLOR, *ibid* **39** (1968) 3717.
11. A. SAGAR and J. W. FAUST, *ibid* **38** (1967) 482.
12. *Idem, ibid* **38** (1967) 2240.
13. V. M. KOSEVICH, *Soviet Phys. Crystallog.* **5** (1961) 715.
14. T. HATTORI, *J. Phys. Soc. Japan* **24** (1968) 762.
15. Y. ECKSTEIN, A. W. LAWSON, and D. H. RENEKER, *J. Appl. Phys.* **31** (1960) 1534.
16. R. D. BROWN, R. L. HARTMAN, and S. H. KOENIG, *Phys. Rev.* **172** (1968) 598.
17. N. G. PACE, G. A. SAUNDERS, and Z. SÜMENGEN, *J. Phys. Chem. Solids* **31** (1970) 1467.
18. A. P. JEAVONS and G. A. SAUNDERS, *Proc. Roy. Soc.* **A310** (1969) 415.
19. Ö. ÖKTÜ and G. A. SAUNDERS, *Proc. Phys. Soc.* **91** (1967) 156.
20. J. P. MICHENAUD, J. M. STREYDIO, J. P. ISSI, and A. LUYCKX, *Solid State Commun.* **8** (1970) 455.

Received 16 November 1970 and accepted 24 February 1971.